

Diffusion-based Adversarial Purification for Intrusion Detection

Mohamed Amine Merzouk^{1,2}, Erwan Beurier^{1,2}, Reda Yaich², Nora Boulahia-Cuppens¹, and Frédéric Cuppens¹

¹ Polytechnique Montréal, Montréal, Canada
 {mohamed-amine.merzouk,erwan.beurier,
 nora.boulahia-cuppens,frederic.cuppens}@polymtl.ca
² IRT SystemX, Palaiseau, France
 {mohamed-amine.merzouk,erwan.beurier,
 reda.yaich}@irt-systemx.fr

Abstract. The escalating sophistication of cyberattacks has encouraged the integration of machine learning techniques in intrusion detection systems, but the rise of adversarial examples presents a significant challenge. These crafted perturbations mislead ML models, enabling attackers to evade detection or trigger false alerts. In response, adversarial purification has emerged as a compelling solution, particularly with diffusion models showing promising results. However, their purification potential remains unexplored in the context of intrusion detection. This paper demonstrates the effectiveness of diffusion models in purifying adversarial examples in network intrusion detection. Through a comprehensive analysis of the diffusion parameters, we identify optimal configurations maximizing adversarial robustness with minimal impact on regular performance. Importantly, this study reveals insights into the relationship between diffusion noise and diffusion steps, representing a novel contribution to the field. Our experiments are carried out on two datasets and against five adversarial attacks. The implementation code is publicly available.

Keywords: Adversarial defense · Adversarial purification · Adversarial examples · Diffusion models · Intrusion detection.

1 Introduction

Intrusion detection stands out as one of the most formidable challenges in cybersecurity, especially with the increasing sophistication of cyberattacks. Unfortunately, traditional signature-based approaches reach their limit against previously unknown threats, also called zero-days. As such, the integration of Machine Learning (ML) techniques has emerged as a promising avenue for enhancing the detection capabilities of intrusion detection systems.

However, the advent of adversarial examples [27,5] poses a severe obstacle to the reliability of ML, specifically in critical tasks such as intrusion detection. They are generated from regular data instances by adding a meticulously crafted

perturbation that misleads an ML model. Applied to network data, they enable cyber attackers to either evade ML-based intrusion detection systems or flood the network with false alerts.

In response to the escalating threat of adversarial attacks, research efforts have been directed toward designing effective countermeasures. Among the various defensive approaches, adversarial purification has emerged as a compelling solution to remove the adversarial perturbation from data before processing it. This defense is particularly interesting for intrusion detection, as it can be integrated upstream of the model without retraining. Recent work [18] has demonstrated promising purification performance using diffusion models [22,8].

Diffusion models are generative models inspired by the dynamics of diffusion processes in physics [22]. They consist of a forward process that gradually adds noise to initial data and a backward process that reconstructs that data using a deep neural network. Because diffusion models are trained using examples drawn from the original data distribution, the reconstructed data is expected to adhere to the same distribution, even when the initial data is an adversarial example. Thus, they can be used for adversarial purification: removing the perturbation from adversarial examples to classify them correctly. Furthermore, since they are not explicitly trained on adversarial examples, their purification performance is not limited to a specific adversarial attack.

Despite the recent attention given to adversarial purification with diffusion models, there remains a notable gap in understanding their potential in the context of intrusion detection. This paper fills that gap by studying the purification effects of diffusion models and demonstrating their effectiveness on network intrusion detection. By conducting a comprehensive analysis of the diffusion parameters, we identify optimal configurations maximizing the adversarial robustness with limited impact on the regular performance. We show the effectiveness of our method on two network datasets (UNSW-NB15 [17] and NSL-KDD [29]) and against state-of-the-art adversarial attacks. Moreover, to our knowledge, this is the first investigation of the relationship between the number of diffusion steps and the optimal amount of diffusion noise for adversarial purification. Our findings demonstrate that the optimal amount of diffusion noise depends not on the number of diffusion steps but rather on the amount of adversarial perturbation.

Section 2 introduces the background and related works in cybersecurity. In Section 3, we describe the experiment methodology. We report the results in Section 4, followed by a discussion in Section 5 and a conclusion in Section 6.

2 Background and Related Work

This section introduces the major approaches to adversarial defense, provides some background on diffusion models, and reviews the literature on diffusion models in intrusion detection systems and adversarial purification.

Adversarial Defenses. The following presents three dominant approaches to defend against adversarial examples [34].

Adversarial training consists of training the model with adversarial examples in addition to the training data [5,14]. Despite its effectiveness, this technique has several drawbacks: (i) it requires the retraining of the model and significantly lengthens the training duration, and (ii) it protects only against adversarial examples generated with the methods it was trained on.

Adversarial detection consists of a separate classifier deployed upstream of the ML model that detects and discards adversarial examples before they are fed to the model [1]. It is plug-and-play and does not require retraining. Several supervised and unsupervised techniques exist; interested readers may refer to [1] for a detailed review. Unfortunately, adversarial detection also depends on the adversarial attacks on which it was trained. Moreover, since it is a classifier, it can be fooled to some extent [2].

Adversarial purification consists of a separate model deployed upstream of the ML model that removes the perturbation from adversarial examples before they are fed to the model [24,26]. This approach is also plug-and-play, and the purification models are typically trained independently of the ML model. Adversarial purification does not require retraining, and it is, in many cases, independent of the adversarial attacks. This paper focuses on the adversarial purification approach using diffusion models [18].

Diffusion Models. Diffusion models are a class of generative models that leverage the diffusion processes used in physics to learn complex data distributions and samples from them [22,8]. Instead of modeling the distribution like VAEs [10] and GANs [4], they model the process of transforming a simple distribution (e.g., Gaussian noise) into the target distribution through a sequence of steps. They consist of two Markov processes: a *forward* and a *reverse* process.

In the *forward process*, each step involves adding Gaussian noise to the data over T steps until no structure remains; it corresponds to a smooth transition from the complex data distribution to a Gaussian distribution (latent space). The amount of noise added at each step depends on the variance schedule β . In the *reverse process*, each step reverts the corresponding forward step—removes the diffusion noise—to reconstruct the original data distribution. Since the reverse process is mathematically intractable, it is approximated with deep neural networks. In this work, we use discrete diffusion steps, but the continuous case can also apply; it requires solving stochastic differential equations [25].

In the following, we provide the intuition into the theory behind diffusion models. We consider a dataset x_0 with unknown distribution $x_0 \sim q(x_0)$. For a given number T of steps, we consider the Markov chain $(x_t)_{t \leq T}$ with transitions

$$q(x_{t+1}|x_t) = \mathcal{N}\left(x_{t+1}; \sqrt{1 - \beta_{t+1}}x_t, \beta_{t+1}I_n\right), \quad (1)$$

that is, we gradually add Gaussian noise with a given variance $(\beta_t)_{t \leq T}$ to the data. If we define $\bar{\alpha}_t = \prod_{i=1}^{i=t} (1 - \beta_i)$, then the cumulative noise addition from the clean data to step t is written:

$$q(x_t|x_0) \simeq \mathcal{N}\left(x_t; \sqrt{\bar{\alpha}_t}x_0, (1 - \bar{\alpha}_t)I_n\right). \quad (2)$$

Equation 2 describes the *forward process* of diffusion models. Note that to ensure the diversity of generated data the variance schedule should guarantee that the data resembles a Gaussian distribution at the end of the forward process:

$$q(x_T|x_0) \simeq \mathcal{N}(x_T; 0, I_n). \quad (3)$$

The *reverse process* consists of generating examples from the original data distribution using the reverse Markov chain; it starts from a Gaussian distribution with transitions

$$p(x_t|x_{t+1}) = \mathcal{N}(x_{t+1}; \mu_\theta(x_t, t), \Sigma_\theta(x_t, t)), \quad (4)$$

where θ represents the parameters of the deep neural network used to estimate the diffusion noise to be removed.

Adversarial Purification with Diffusion Models. Adversarial purification is the process of removing the perturbation from adversarial examples to classify them correctly. This process can be seen as a generative task and approached with diffusion models. The gradual addition of Gaussian noise in the forward step submerses the adversarial perturbation, but the data becomes too noisy to be correctly classified. Thus, the reverse step reconstructs the data in the original distribution without adversarial perturbations.

Furthermore, the forward process does not need to complete T steps and reach a Gaussian distribution. There should be enough added noise to submerge the adversarial perturbation, but not too much, as it damages the data structure and decreases the accuracy. The forward process should stop at the optimal diffusion step t^* , where the diffusion noise suffices to remove the adversarial perturbation while preserving the structure for the classification [18].

After this concept was introduced in [18], later work leveraged guided diffusion models for adversarial purification [30,32]. Authors in [12] train a robust guidance with an adversarial loss and apply it to the reverse process. Diffusion models are also used to purify backdoors in poisoned models [21].

Diffusion Models in Intrusion Detection. Intrusion detection systems benefit greatly from the automation provided by ML, including deep learning [13,23,7]. However, network intrusion datasets are often imbalanced; benign traffic outweighs malicious traffic. Due to their generative capabilities, diffusion models are successfully applied in data augmentation for balancing network datasets [35,28,6]. The diffusion model can also detect intrusion by learning the distribution of benign traffic. The difference between the original and reconstructed data is then used to detect malicious traffic [31,33].

However, to our knowledge, no prior research has investigated the adversarial purification potential of diffusion models in the context of intrusion detection. This paper represents the foremost initiative to address diffusion-based adversarial purification in intrusion detection.

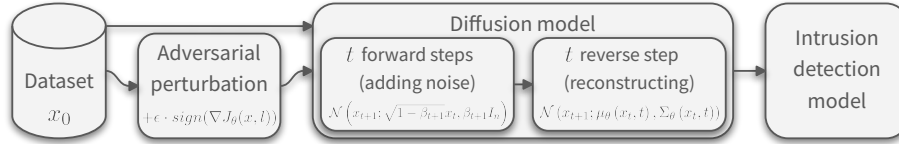


Fig. 1: Methodology scheme: dataset instances x_0 undergo adversarial perturbation, the diffusion model’s purification, and then the intrusion detection classification.

3 Methodology

As shown in Figure 1, our methodology consists of a diffusion model deployed upstream of the intrusion detection model. The diffusion model serves as a "filter" that removes adversarial perturbations. It adds noise to the data for several steps t and reconstructs it through the reverse diffusion process involving the diffusion neural network. The data, whether original or adversarial, are first purified by the diffusion model and then fed to the intrusion detection model to determine if they are benign or malicious.

The intrusion detection model is a fully connected neural network with fixed hyperparameters throughout the experiments. It comprises a fully connected neural network with 5 hidden layers of 256, 512, 1024, 512, and 256 Rectified Linear Units (ReLU). It is trained for 10,000 epochs, and the parameters are optimized using Adam with a learning rate of 10^{-5} .

The diffusion models are trained according to [8, Algorithm 1]. We consider T discrete diffusion steps. Instead of having a separate neural network for each timestep [22], we encode the timesteps as sinusoidal embeddings and add them to each layer of the diffusion neural network [8].

The purification results are recorded across the diffusion steps. For each $t \in [1, T]$, we apply t forward diffusion steps to the data instance x_0 to get x_t ; then we apply t reverse diffusion steps to x_t to get \hat{x}_0 , the reconstruction of x_0 .

The variance schedule β is linearly distributed (T evenly spaced values between β_1 and β_T). Across different experiments, the number of diffusion steps T is 100 or 1000, while β_1 varies between 10^{-5} and 10^{-4} , and β_T varies between 10^{-4} and 10^{-1} .

The diffusion neural networks are fully connected neural networks with 10 hidden layers; each hidden layer typically consists of 960 ReLU units, except for the experiments that compare neural network architectures. The diffusion neural networks are trained for 200,000 epochs, where each epoch consists of predicting a random step of the reverse process for each dataset instance. The loss function is a Mean Squared Error (MSE), and the parameters are optimized using AdamW with a learning rate of 10^{-4} .

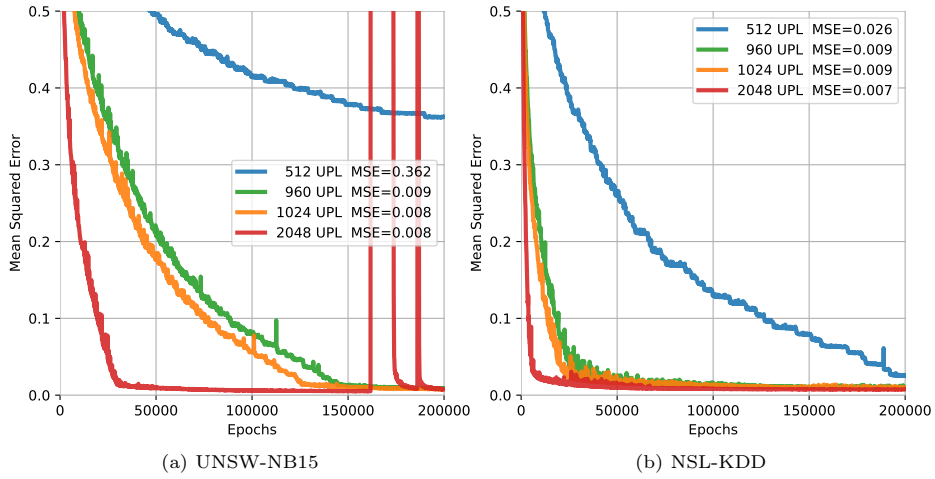


Fig. 2: Reconstruction loss over training epochs for different neural network sizes

The metrics recorded during the experiments evaluate two aspects of diffusion models: (i) the reconstruction performance by recording the reconstruction loss (MSE between the original data and the reconstructed data) for a diffusion step t , and (ii) the adversarial purification performance by feeding the reconstructed data to the intrusion detection model and recording its accuracy.

The optimal diffusion step $t^* \in [1, T]$ is the step that maximizes the intrusion detection accuracy on adversarial examples [18]. It should be large enough to dilute the adversarial perturbation with diffusion noise. However, the larger it is, the more data structure it dilutes, which decreases the test accuracy.

All experiments are carried out on two prominent network datasets: NSL-KDD [29], which is old but still widely used for benchmarking and comparison, and UNSW-NB15 [17] which is more recent and representative of modern network traffic [20]. For further details on the implementation of our experiments, we make our code publicly available ³.

4 Results

In this section, we present the results of our experiments. We first analyze the reconstruction loss throughout the training of the diffusion models to identify optimal hyperparameters. Then, we study the reconstruction loss and the accuracy of the intrusion detection model on reconstructed data. We compare the robustness of the intrusion detection model with respect to the level of diffusion applied to the data. We aim to find the optimal diffusion step t^* that removes the adversarial perturbation and increases the robustness while minimizing the repercussions on non-adversarial data.

³ <https://github.com/mamerzouk/adversarial-purification>

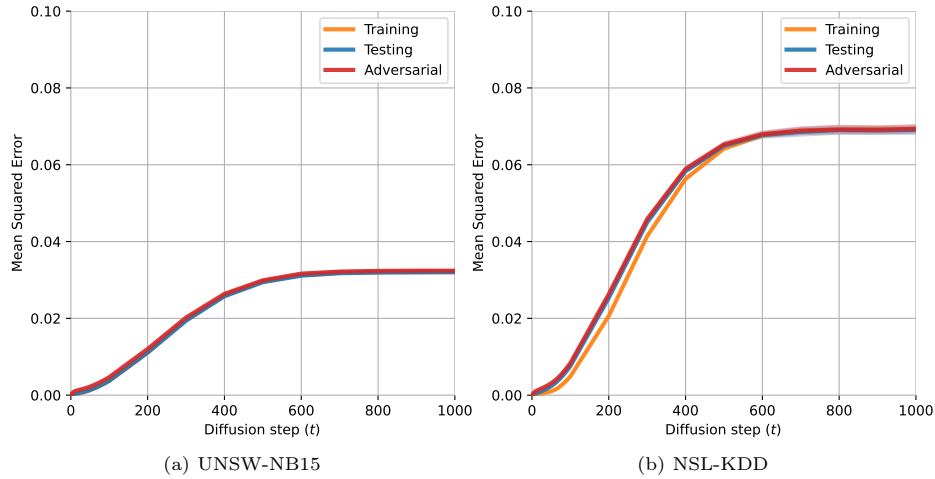


Fig. 3: Reconstruction loss over the diffusion steps t

Furthermore, we analyze the impact of several diffusion parameters on the purification performance: the number of steps T , the initial variance β_1 , and the final variance β_T . Finally, we study the impact of the adversarial perturbation amplitude ϵ on the optimal diffusion step t^* and compare our purification model against five state-of-the-art adversarial attacks. The figures present the results on both UNSW-NB15 and NSL-KDD; the values are the mean and standard deviation over 10 randomly initialized runs.

Unless otherwise noted, the diffusion models in these experiments use the standard diffusion parameters proposed in the previous work [8]: $\beta_1 = 10^{-4}$, $\beta_T = 0.02$, and $T = 1000$.

Diffusion neural network size. Here, we analyze the training of diffusion models on network data. We specifically compare the impact of the size of the diffusion neural network on the training loss. We elaborate further on the impact of the number of diffusion steps on the training loss in Appendix A. Figure 2 shows the reconstruction loss (in MSE) over the training epochs for different Units Per Layer (UPL). We observe that the reconstruction loss decreases earlier for larger diffusion neural networks. Furthermore, larger neural networks reach lower MSE values when they stabilize, 0.008 and 0.007 with 2048 UPL against 0.362 and 0.026 with 512 UPL on UNSW-NB15 and NSL-KDD, respectively. This is due to the capacity of larger neural networks to model more complex patterns and learn better representations of the data. However, larger models have drawbacks; they take significantly longer to train and require more computational power. Larger models also display instabilities during the training; Figure 2 shows how the 2048 UPL diffusion model loss peaks randomly between 150,000 and 200,000 epochs on UNSW-NB15. For the rest of the experiments,

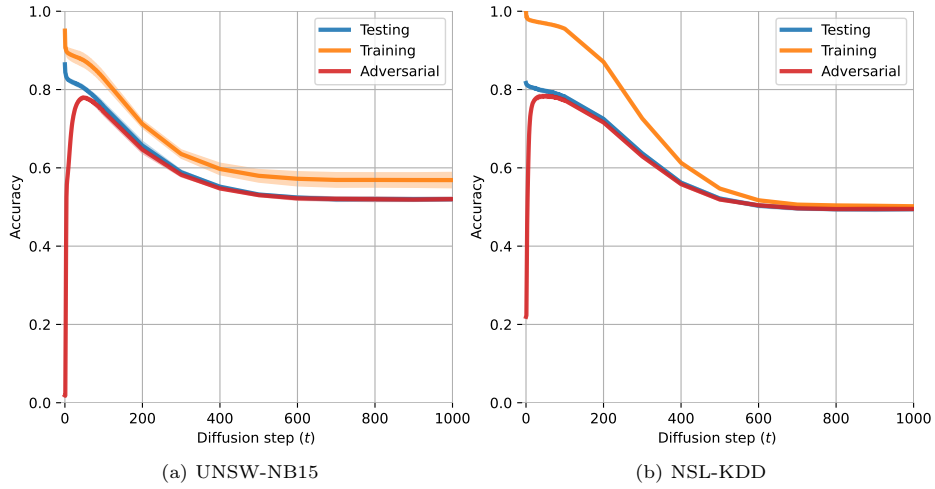


Fig. 4: Intrusion detection accuracy over the diffusion steps t

we will rely on diffusion neural networks with 10 hidden layers of 960 UPL trained for 200,000 epochs.

Reconstruction loss and accuracy over t . Figure 3 shows the reconstruction loss over the diffusion steps t , while Figure 4 shows the accuracy of the intrusion detection model on the same reconstructed data over the diffusion steps t .

Figure 3 shows that the reconstruction loss increases similarly for all three sets, the lines even overlap on UNSW-NB15. Indeed, as noise is added gradually, the data structure is slowly destroyed. The more diffusion steps are applied, the more noise is added, and the harder it is to reconstruct precisely the data. After 600 steps, the reconstruction loss plateaued around 0.03 and 0.07 on UNSW-NB15 and NSL-KDD, respectively. Moreover, we notice that the reconstruction loss on adversarial examples is slightly superior to that on the original testing set. The difference in the reconstruction losses can also be used as an indicator for detecting adversarial examples. This avenue is not investigated in this paper, as adversarial detection approaches are out of our scope.

The accuracy curve in Figure 4 corroborates the previous results: the training and testing accuracy decrease as the diffusion step increases due to the damaged data structure. It becomes more challenging for the intrusion detection model to distinguish benign and malicious traffic, which decreases its accuracy. After 600 steps, the reconstructed data is too noisy to be classified correctly.

Purification performance. In order to evaluate the robustness of the intrusion detection after the diffusion model’s purification, we focus on the red line in Figure 4, which represents the accuracy of the intrusion detection model on adversarial examples. Those adversarial examples were generated from the testing

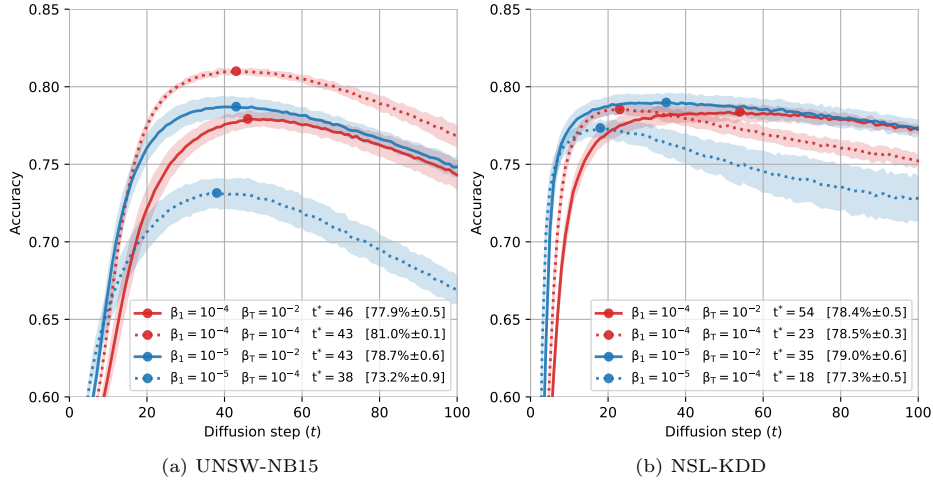


Fig. 5: Intrusion detection accuracy over diffusion step t for different β_1 . Continuous lines for $\beta_T = 10^{-2}$ and dotted lines for $\beta_T = 10^{-4}$. The marker indicates the maximum accuracy reached at the optimal diffusion step t^* .

set using the targeted Fast Gradient Sign Method (FGSM) with a perturbation amplitude $\epsilon = 0.03$. At step 0, before purification, the accuracy on adversarial data is 0.02, while it is 0.86 on the original test data, indicating that the adversarial attack succeeded in misleading the intrusion detection model. After a few diffusion steps, the adversarial accuracy increases drastically. The added diffusion noise dilutes the adversarial perturbation that misleads the model while preserving enough data structure for a good classification. After 44 steps, the adversarial accuracy peaks at 78% while the test accuracy is 80%. This diffusion step t^* is optimal as it maximizes the accuracy on adversarial examples while minimizing the impact on the non-adversarial test data. This result empirically shows the purification capabilities of diffusion models in intrusion detection.

After the peak, the structure damage due to the addition of diffusion noise decreases the adversarial accuracy. Since the adversarial perturbation has been removed, the difference between the test and adversarial accuracy disappears; it is below 0.01 after $t = 90$. Both values decrease until they reach random classification when the reconstructed data is too noisy.

Variance schedule. The variance of the Gaussian noise added at step t of the diffusion process is denoted β_t . It follows a linear distribution of T evenly spaced values between β_1 and β_T . The variance schedule is an essential parameter of the diffusion process; we hypothesize that it is also critical to the purification capabilities of diffusion models. In the following, we study the impact of the variance schedule β on the purification capabilities of the diffusion model through the accuracy of the intrusion detection model on purified examples. Using a fixed $T = 1000$, we vary both β_1 and β_T to find an optimal schedule.

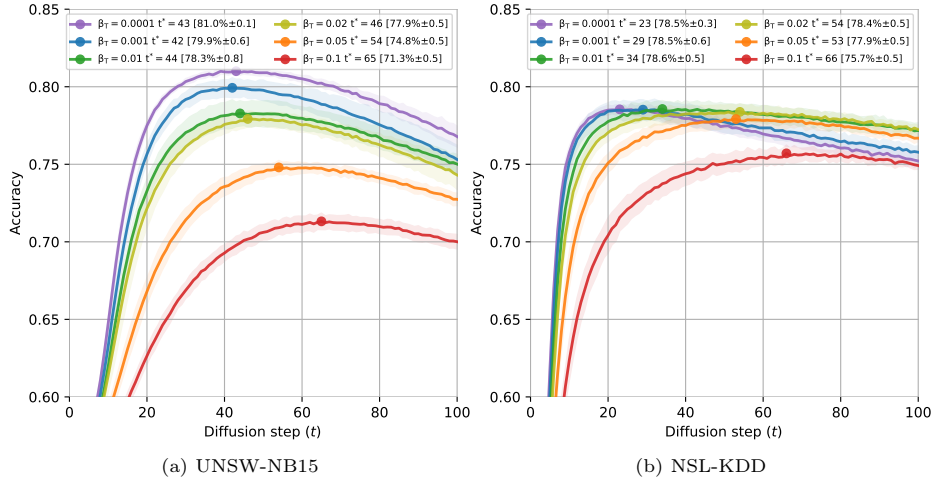


Fig. 6: Intrusion detection accuracy over diffusion step t for different β_T

Figure 5 shows the impact of β_1 , the first value of the variance schedule. If we focus on the continuous lines, corresponding to $\beta_T = 10^{-2}$, we do not see a significant difference between the two values of β_1 . However, with a smaller β_T , the difference between β_1 becomes significant. The dotted lines, corresponding to $\beta_T = 10^{-4}$, show a large difference between the two values of β_1 . As the final β decreases, the difference between the accuracy of the two β_1 values increases. The impact of the initial variance β_1 is therefore linked to the length of the variance schedule $\beta_T - \beta_1$ and becomes less significant as the interval increases. This result suggests that β_T plays an influential role in the purification.

Figure 6 shows the impact of β_T , the final variance of the diffusion schedule. The figure shows an increasing accuracy with smaller β_T values. The intuition is that as β_T decreases, the interval between successive variance values decreases, which makes the noising more gradual and easier for the neural network to reconstruct. On UNSW-NB15, the maximum accuracy value is 81% ± 0.1 at $t^* = 43$, it was reached with the smallest value $\beta_T = 10^{-4}$, which represents a constant variance schedule (since $\beta_1 = 10^{-4}$). On NSL-KDD, the maximum accuracy value is very close between when $\beta_1 \leq 10^{-2}$, but $\beta_1 \leq 10^{-4}$ is the earliest to achieve 78.5 ± 0.3 after only $t^* = 23$.

Number of diffusion steps T . In addition to the initial and final perturbation values β_1 and β_T , the diffusion process is characterized by the number of diffusion steps T . This parameter determines the granularity of the diffusion since a larger number of steps T makes the step size smaller.

In the following, we study how the number of diffusion steps T affects the optimal diffusion steps t^* . We compare diffusion models with $T = 100$ and $T = 1000$ with respect to the optimal diffusion step t^* and identify how it translates to an equivalent amount of noise. In Appendix A, we further investigate the

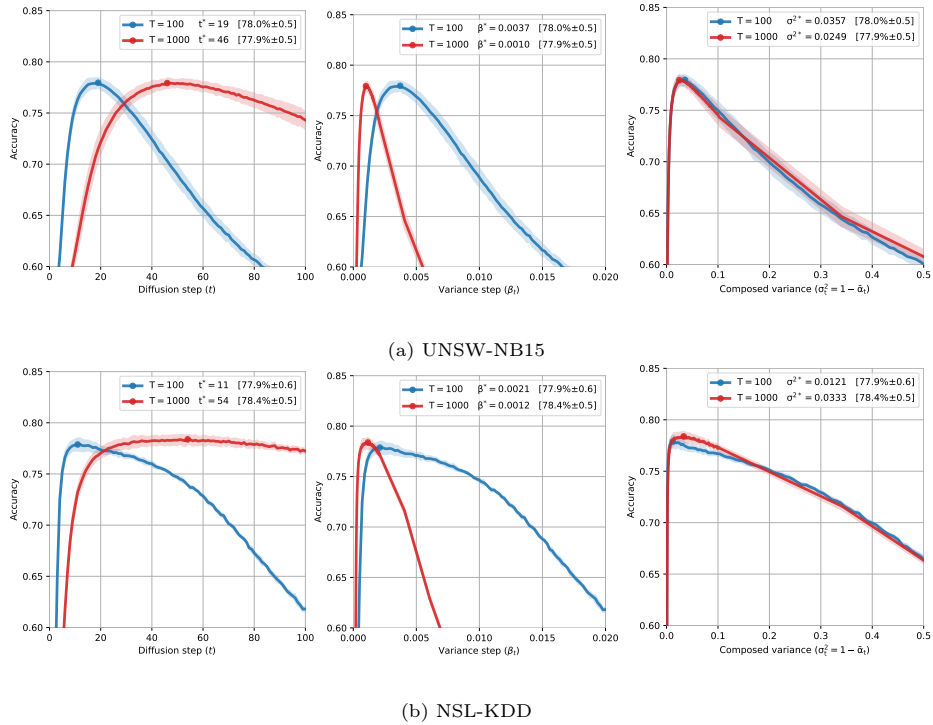


Fig. 7: Intrusion detection accuracy over t , β_t , and σ_t^2 for different number of diffusion steps T

impact of the number of diffusion steps T on the training loss and the purification performance with the optimal variance schedule.

Figure 7 shows the impact of the number of diffusion steps T over three references: the diffusion step t , the variance step β_t , and the composed variance σ_t^2 . This experiment uses the standard diffusion parameters to focus the analysis on when the optimum is recorded rather than its value. With the optimal variance interval recorded in Figure 6, $\beta_1 = \beta_T = 10^{-4}$, the 1000-step diffusion model largely over-performs the 100-step one on UNSW-NB15, as shown in Figure 11 (Appendix A).

In the first part of Figure 7, we see the accuracy across the diffusion step t . The $T = 100$ diffusion model reaches its optimum at $t^* = 19$ and $t^* = 11$, while the $T = 1000$ reaches its optimum at $t^* = 46$ and $t^* = 54$ on UNSW-NB15 and NSL-KDD, respectively. This indicates a slower evolution when $T = 1000$, which is coherent since the variance steps are smaller. Therefore, we plot the same values with respect to the variance steps β_t to find a similarity. In the second part of Figure 7, the x-axis corresponds to β_t and covers the whole interval from 0 to $\beta_T = 0.02$. However, the optimum is still reached at distant values of β . For $T = 100$, it is reached with $\beta^* = 0.0037$ and $\beta^* = 0.0021$, while for $T = 1000$, it

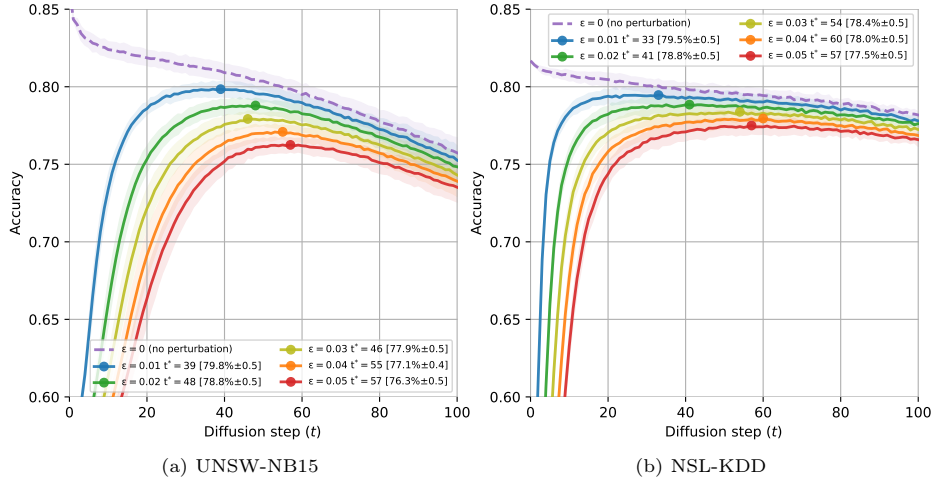


Fig. 8: Intrusion detection accuracy over the diffusion step t for different adversarial perturbation amplitudes ϵ generated with FGSM

is reached with $\beta^* = 0.0010$ and $\beta^* = 0.0012$ in UNSW-NB15 and NSL-KDD, respectively.

β_t is the amount of variance applied at the diffusion step t , but it does not correspond to the total variance applied to the initial data x_0 . Indeed, the diffusion forward process is a composition of Gaussian distributions with gradual variances β_t . The total (composed) variance σ_t^2 of such composition is the sum of the individual variances, $\sigma_t^2 = 1 - \bar{\alpha}_t$ (Equation 2).

The third part of Figure 7 shows the accuracy across the composed variance σ_t where the two lines overlap, indicating a similar accuracy regardless of the number of diffusion steps T . The optimum is reached at $\sigma_t^2 = 0.0249$ and $\sigma_t^2 = 0.0333$ for $T = 1000$, and $\sigma_t^2 = 0.0357$ and $\sigma_t^2 = 0.0121$ for $T = 100$ on UNSW-NB15 and NSL-KDD, respectively. Considering the scale of σ_T^2 in Figure 7, the optimum values are relatively close. We note from this experiment that the optimal noise added σ^{2*} approaches 0.03, which corresponds to the adversarial perturbation amplitude ϵ used in these experiments. This result suggests a dependence between the optimal noise amount and the perturbation amplitude.

Adversarial perturbation amplitude ϵ . Beyond the diffusion parameters, the purification performance of diffusion models depends on the amount of adversarial perturbation ϵ added to the data. Figure 8 shows the accuracy of the intrusion detection model on increasing ϵ values. It demonstrates how the purification performance decreases as the perturbation amplitude increases. The accuracy at t^* goes from 79.8% ± 0.5 and 79.5% ± 0.5 when $\epsilon = 0.01$ to 76.3% ± 0.5 and 77.5% ± 0.5 when $\epsilon = 0.05$ on UNSW-NB15 and NSL-KDD, respectively. Another pattern is that it takes more diffusion steps to reach an optimum as ϵ increases. The two phenomena are linked: the diffusion model needs to add more

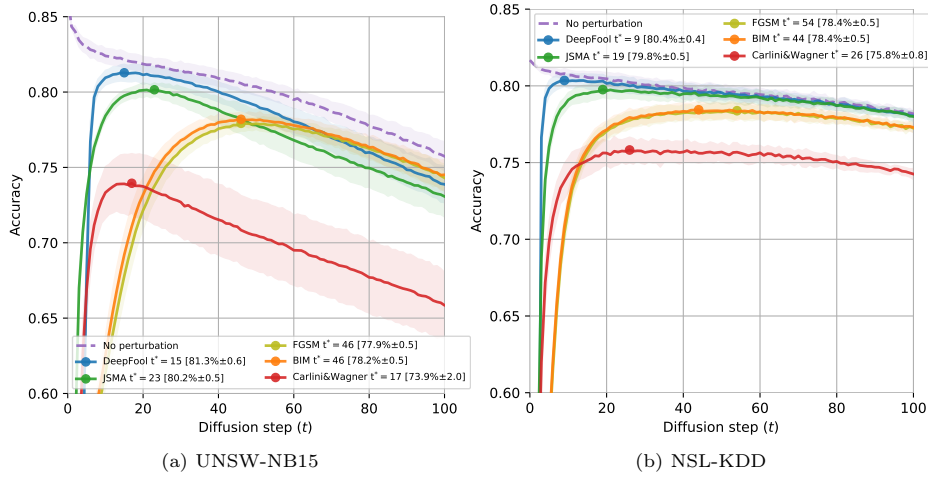


Fig. 9: Accuracy over the diffusion step t for different adversarial attacks

perturbation to dilute a larger ϵ , thus taking more diffusion steps. However, the test accuracy (purple line) decreases as more noise is added. Since it represents an upper bound on the adversarial accuracy, it causes the optimal adversarial accuracy to decrease as ϵ increases.

Adversarial attacks. The efficiency of adversarial examples also depends on the method used to generate them. Various methods exist, each optimizing different distance norms and criteria. While previous experiments show how diffusion models considerably improve the adversarial accuracy of intrusion detection models, they have only been tested on one adversarial attack (FGSM). Here, we study how the purification performance is generalized to other adversarial examples’ generation methods. We compare five well-established methods, namely: DeepFool [16], Jacobian-based Saliency Map Attack (JSMA) [19], Fast Gradient Sign Method (FGSM) [5], Basic Iterative Method (BIM) [11], and Carlini&Wagner’s L_2 attack [3].

Figure 9 shows the adversarial accuracy of the intrusion detection model for the adversarial attacks and the testing set baseline. We note that the diffusion models successfully purify adversarial examples from all 5 generation methods. However, the optimal adversarial accuracy and diffusion step vary from one method to the other. Carlini&Wagner’s attack is the most resistant to adversarial purification, with a maximum adversarial accuracy of $73.9\% \pm 2$ and $75.8\% \pm 0.8$ on UNSW-NB15 and NSL-KDD, respectively. The optimum is reached after only 17 steps on UNSW-NB15, 2.7 times faster than FGSM. On NSL-KDD, the adversarial accuracy is stable between 30 and 100, making t^* less accurate.

FGSM and BIM achieve similar performance; FGSM reaches a maximum of $77.9\% \pm 0.5$ and $78.4\% \pm 0.5$, while BIM reaches a maximum of $78.2\% \pm 0.5$ and $78.4\% \pm 0.5$ on UNSW-NB15 and NSL-KDD, respectively. The optimal diffu-

sion steps are also very close between the two. This similarity is explained by the fact that BIM is based on FGSM; it applies small FGSM steps iteratively (100 in our experiments) to optimize the adversarial examples. However, the iterative approach does not make BIM’s adversarial examples more robust to our diffusion-based adversarial purification. The diffusion models achieve the highest purification performance on DeepFool’s adversarial examples, with a maximum accuracy of $81.3\% \pm 0.6$ and $80.4\% \pm 0.4$ on UNSW-NB15 and NSL-KDD, respectively, closely followed by JSMA with a maximum accuracy of $80.2\% \pm 0.5$ and $79.8\% \pm 0.5$ on UNSW-NB15 and NSL-KDD, respectively. DeepFool and JSMA also had the fastest-growing adversarial accuracy values among other attacks, almost reaching the testing accuracy upper bound.

5 Discussion

Diffusion neural network. The size of the neural network has a considerable impact on the reconstruction loss of the diffusion model. Larger neural networks converge faster and reach lower reconstruction loss values due to their capacity to model more complex patterns and learn better representations. The main obstacle to using larger neural networks is that they take longer to process the data, making the training and reconstruction longer. The diffusion neural network should be hyperparameterized with particular attention to domain-specific time constraints, especially in network intrusion detection, where the reaction time is critical.

In addition to the size of the diffusion neural network, other hyperparameters impact the reconstruction loss and, potentially, the purification performance. The choice of the loss function, the optimization algorithm, and the learning rate affect the convergence time and help find better optimums. Finally, fully connected neural networks can be replaced with more sophisticated neural network architectures that model the diffusion process more precisely. In sum, optimizing diffusion neural networks is a promising avenue for improving the reconstruction loss, the purification performance, and even the processing time of diffusion models.

Variance schedule β . The variance schedule determines the amount of noise added at each step of the forward diffusion process. In the experiments, the schedule is linear—it consists of T evenly spaced values between β_1 and β_T . This schedule is essential for adversarial purification, since adding too little noise does not remove the adversarial perturbation, and too much noise corrupts the data structure. The importance of β_1 , the variance of the first diffusion step, depends on the total length of the diffusion schedule $\beta_T - \beta_1$. When the schedule is small, the choice of the starting value makes a considerable difference in the purification capabilities. As the difference between β_1 and β_T increases, β_1 is less significant since it has little impact on the rest of the variance values.

On the other hand, the last value β_T has a more significant impact on the variance schedule, which also extends to the purification performance. In the

standard setting, where $T = 1000$, $\beta_1 = 10^{-4}$, and $\beta_T = 0.02$, a smaller value of β_T leads to a better adversarial accuracy. The best purification performance was recorded with the smallest value $\beta_T = \beta_1 = 10^{-4}$, which describes a constant variance schedule.

As opposed to generative models, diffusion models in adversarial purification do not require the forward process to reach a Gaussian distribution $\mathcal{N}(x_T; 0, I_n)$ after T steps. Therefore, there is more freedom in choosing the diffusion parameters to optimize the adversarial accuracy.

Number of diffusion steps T . The number of diffusion steps affects multiple aspects of the diffusion process. It determines the size of the variance schedule β and its values since there are T evenly spaced values. In the best-performing case $\beta_T = \beta_1 = 10^{-4}$, the number of diffusion steps makes a considerable difference in favor of a larger T . Having the same variance schedule divided into more variance steps allows the neural network to learn more details about the applied noise, which are then helpful to accurately reconstruct the data in the reverse process.

The number of diffusion steps also affects the optimal diffusion step t^* ; it happens earlier in the process when T is smaller. This is explained by the fact that the diffusion steps t do not correspond to an equivalent variance step β_t . However, even when considering β_t instead of t , the reconstruction curve does not match. This is because the β_t values are gradually added to the data (Equation 1) according to the variance step; they do not represent the total variance applied to the data. Instead, we consider the variance of the composition, $\sigma_t^2 = 1 - \bar{\alpha}$, which makes the values of $T = 100$ and $T = 1000$ match. The total variance that maximizes the adversarial accuracy, σ^{2*} is very close between the two different T values. Furthermore, the optimal variance σ^{2*} approaches the value of the perturbation amplitude ϵ , demonstrating the dependence of the diffusion noise on the adversarial perturbation.

In sum, diffusion models with more diffusion steps achieve better adversarial accuracy with an optimal variance schedule. However, it takes more steps to reach optimum, translating into a longer purification time. Thus, the choice of T should also consider the time constraints that characterize the application domain.

Adversarial perturbation amplitude. The diffusion-based adversarial purification effectively removes adversarial perturbations from network traffic data. However, the effectiveness of this method varies slightly depending on the nature of the adversarial examples. In the case of adversarial examples generated with FGSM, the parameter ϵ determines the amount of perturbation added to the data. As the ϵ increases, more noise is required to dilute the perturbation, making the optimum occur later in terms of diffusion steps. Another side effect is that the extra required noise also dilutes some of the data structure, thus decreasing the test accuracy, representing an upper bound to the adversarial accuracy. Therefore, the maximum adversarial accuracy decreases as ϵ increases.

Adversarial attacks. In addition to the perturbation amplitude ϵ , the purification process is sensitive to the adversarial examples’ generation method. The results show a considerable gap in the adversarial accuracy between different methods. In particular, DeepFool and JSMA are easier to purify and approach the test accuracy upper-bound after a few diffusion steps, FGSM and BIM achieve close performance due to their similarities, and Carlini&Wagner’s L_2 attack is the most resistant but our method still recovers up to 75% of the accuracy.

Adversary’s constraints. The adversarial examples’ generation method and the adversarial perturbation amplitude are both parameters controlled by the adversary when they generate the adversarial examples. However, they are constrained in the amount of perturbation they can add. A larger adversarial perturbation can increase the chances of being detected, cancel the purpose of the data, or even break its consistency, especially for highly structured data like network traffic [15]. In the experiments, we consider the worst-case scenario where the attacker perturbs all the data features. However, the design of real-world diffusion-based adversarial purification models should consider a realistic threat model to optimize the diffusion parameters.

6 Conclusion

Diffusion models are a promising approach to adversarial purification. Their seamless integration with existing systems and generalization across attack methods make them particularly interesting in the context of intrusion detection.

Throughout this paper, we have demonstrated the effectiveness of diffusion models in mitigating the threat of adversarial examples against intrusion detection. We have compared several diffusion neural network sizes, which show that larger neural networks yield lower loss values despite their increased demands in time and computational resources. Our analysis of the variance schedule indicates the importance of the final variance β_T in determining the purification performance, with smaller values achieving the highest accuracy. Furthermore, we have shown that the optimal amount of diffusion noise σ^{2*} is nearly constant regardless of the number of diffusion steps T and that it approaches the value of the perturbation amplitude ϵ . However, in terms of purification performance, diffusion models with a larger T display better adversarial accuracy despite requiring more diffusion steps. Finally, we benchmarked our method against five state-of-the-art adversarial attacks and an increasing perturbation amplitude.

While scalability and computational complexity remain the main challenges for diffusion models in intrusion detection, especially for inline detection, we envision future research endeavors to refine and optimize diffusion models for practical deployment. As novel adversarial attacks emerge and challenge adversarial defenses [9], our future work will focus on adapting diffusion-based purification to these attacks. Ultimately, complementing diffusion models with other defensive techniques remains necessary to prevent a single point of failure.

Acknowledgments

This work was supported by Mitacs through the Mitacs Accelerate International program and the CRITiCAL chair. It was enabled in part by support provided by Calcul Québec, Compute Ontario, the BC DRI Group, and the Digital Research Alliance of Canada.

References

1. Aldahdooh, A., Hamidouche, W., Fezza, S.A., Déforges, O.: Adversarial example detection for dnn models: A review and experimental comparison. *Artificial Intelligence Review* (2022)
2. Carlini, N., Wagner, D.: Adversarial examples are not easily detected: Bypassing ten detection methods. In: *ACM workshop on artificial intelligence and security* (2017)
3. Carlini, N., Wagner, D.: Towards Evaluating the Robustness of Neural Networks. In: *IEEE Symposium on Security and Privacy (SP)* (2017)
4. Goodfellow, I.J., Pouget-Abadie, J., Mirza, M., Xu, B., Warde-Farley, D., Ozair, S., Courville, A., Bengio, Y.: Generative Adversarial Nets. In: *Advances in Neural Information Processing Systems* (2014)
5. Goodfellow, I.J., Shlens, J., Szegedy, C.: Explaining and harnessing adversarial examples. In: *International Conference on Learning Representations* (2015)
6. Han, F., Ye, P., She, C., Duan, S., Wang, L., Liu, D.: Mmid-bench: A comprehensive benchmark for multi-domain multi-category intrusion detection. *IEEE Transactions on Intelligent Vehicles* (2024)
7. He, K., Kim, D.D., Asghar, M.R.: Adversarial machine learning for network intrusion detection systems: A comprehensive survey. *IEEE Communications Surveys & Tutorials* (2023)
8. Ho, J., Jain, A., Abbeel, P.: Denoising Diffusion Probabilistic Models. In: *Advances in Neural Information Processing Systems* (2020)
9. Kang, M., Song, D., Li, B.: Diffattack: Evasion attacks against diffusion-based adversarial purification. In: *Advances in Neural Information Processing Systems* (2023)
10. Kingma, D.P., Welling, M.: Auto-Encoding Variational Bayes (2022), arXiv:1312.6114
11. Kurakin, A., Goodfellow, I.J., Bengio, S.: Adversarial examples in the physical world. In: *International Conference on Learning Representations* (2017)
12. Lin, G., Tao, Z., Zhang, J., Tanaka, T., Zhao, Q.: Robust Diffusion Models for Adversarial Purification (2024), arXiv:2403.16067
13. Liu, H., Lang, B.: Machine learning and deep learning methods for intrusion detection systems: A survey. *Applied Sciences* (2019)
14. Madry, A., Makelov, A., Schmidt, L., Tsipras, D., Vladu, A.: Towards deep learning models resistant to adversarial attacks. In: *International Conference on Learning Representations* (2018)
15. Merzouk, M.A., Cuppens, F., Boulahia-Cuppens, N., Yaich, R.: Investigating the practicality of adversarial evasion attacks on network intrusion detection. *Annals of Telecommunications* (2022)
16. Moosavi-Dezfooli, S.M., Fawzi, A., Frossard, P.: Deepfool: A simple and accurate method to fool deep neural networks. In: *IEEE Conference on Computer Vision and Pattern Recognition* (2016)

17. Moustafa, N., Slay, J.: Unsw-nb15: a comprehensive data set for network intrusion detection systems (unsw-nb15 network data set). In: 2015 Military Communications and Information Systems Conference (MilCIS) (2015)
18. Nie, W., Guo, B., Huang, Y., Xiao, C., Vahdat, A., Anandkumar, A.: Diffusion Models for Adversarial Purification. In: International Conference on Machine Learning (2022)
19. Papernot, N., McDaniel, P., Jha, S., Fredrikson, M., Celik, Z.B., Swami, A.: The Limitations of Deep Learning in Adversarial Settings. In: IEEE European Symposium on Security and Privacy (EuroS P) (2016)
20. Ring, M., Wunderlich, S., Scheuring, D., Landes, D., Hotho, A.: A survey of network-based intrusion detection data sets. *Computers & Security* (2019)
21. Shi, Y., Du, M., Wu, X., Guan, Z., Sun, J., Liu, N.: Black-box backdoor defense via zero-shot image purification. In: Advances in Neural Information Processing Systems (2023)
22. Sohl-Dickstein, J., Weiss, E., Maheswaranathan, N., Ganguli, S.: Deep Unsupervised Learning using Nonequilibrium Thermodynamics. In: International Conference on Machine Learning (2015)
23. Sohn, I.: Deep belief network based intrusion detection techniques: A survey. *Expert Systems with Applications* (2021)
24. Song, Y., Kim, T., Nowozin, S., Ermon, S., Kushman, N.: Pixeldefend: Leveraging generative models to understand and defend against adversarial examples (2017), arXiv:1710.10766
25. Song, Y., Sohl-Dickstein, J., Kingma, D.P., Kumar, A., Ermon, S., Poole, B.: Score-Based Generative Modeling through Stochastic Differential Equations. In: International Conference on Learning Representations (2021)
26. Srinivasan, V., Rohrer, C., Marban, A., Müller, K.R., Samek, W., Nakajima, S.: Robustifying models against adversarial attacks by langevin dynamics. *Neural Networks* (2021)
27. Szegedy, C., Zaremba, W., Sutskever, I., Bruna, J., Erhan, D., Goodfellow, I., Fergus, R.: Intriguing properties of neural networks. In: International Conference on Learning Representations (2014)
28. Tang, B., Lu, Y., Li, Q., Bai, Y., Yu, J., Yu, X.: A diffusion model based on network intrusion detection method for industrial cyber-physical systems. *Sensors* (2023)
29. Tavallaee, M., Bagheri, E., Lu, W., Ghorbani, A.A.: A detailed analysis of the kdd cup 99 data set. In: IEEE Symposium on Computational Intelligence for Security and Defense Applications (2009)
30. Wang, J., Lyu, Z., Lin, D., Dai, B., Fu, H.: Guided Diffusion Model for Adversarial Purification (2022), arXiv:2205.14969
31. Wang, Y., Ding, J., He, X., Wei, Q., Yuan, S., Zhang, J.: Intrusion detection method based on denoising diffusion probabilistic models for uav networks. *Mobile Networks and Applications* (2023)
32. Wu, Q., Ye, H., Gu, Y.: Guided Diffusion Model for Adversarial Purification from Random Noise (2022), arXiv:2206.10875
33. Yang, C., Wang, T., Yan, X.: Ddmt: Denoising diffusion mask transformer models for multivariate time series anomaly detection (2023), arXiv:2310.08800
34. Yuan, X., He, P., Zhu, Q., Li, X.: Adversarial Examples: Attacks and Defenses for Deep Learning. *IEEE Transactions on Neural Networks and Learning Systems* (2019)
35. Zhang, W., Chen, Z., Chen, D., Li, J., Pan, Y.: Did-ids: A novel diffusion-based imbalanced data intrusion detection system. In: IEEE International Conference on Information, Communication and Networks (ICICN) (2023)

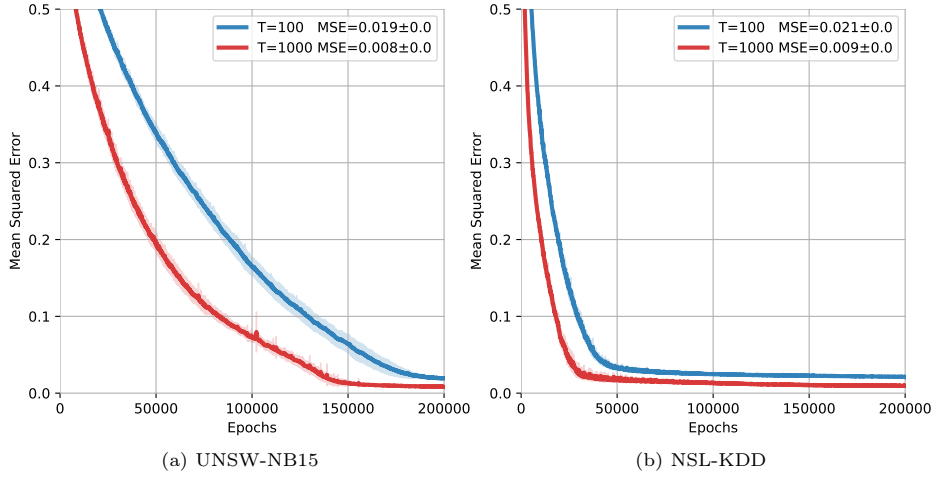


Fig. 10: Reconstruction loss over training epochs for $T = 100$ and $T = 1000$

A More on the number of diffusion steps T

Figure 10 shows the reconstruction loss over the training epochs. Both diffusion models are trained with $\beta_1 = 10^{-4}$, $\beta_T = 10^{-2}$, and a diffusion neural network with 10 hidden layers of 960 ReLU units. We observe that the reconstruction loss for $T = 1000$ is always lower than for $T = 100$. Also, the loss curve for $T = 1000$ stabilizes earlier (around 150,000 epochs as opposed to 190,000 epochs when $T = 100$ on UNSW-NB15). Despite both models having the same β_1 and β_T , a larger T divides the range into smaller steps, allowing for a more gradual noising. As the added noise increases more slowly, the diffusion neural network reconstructs better x_{t-1} at each step.

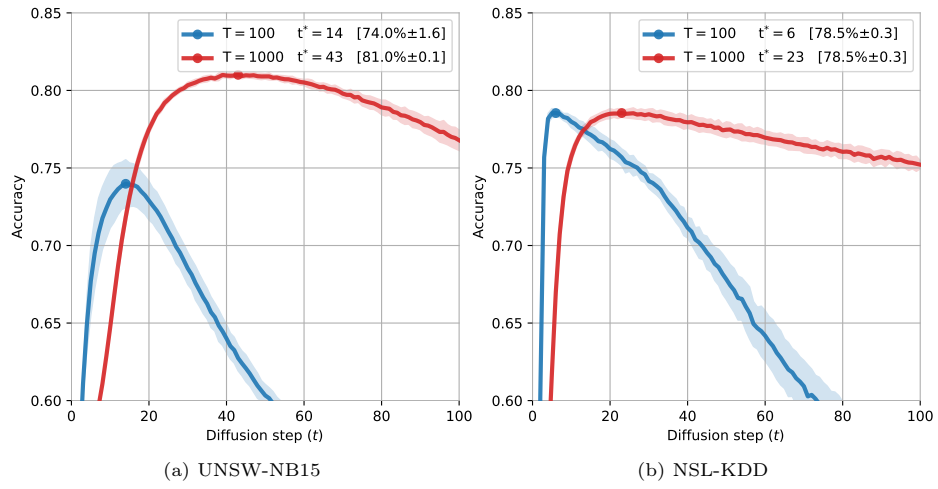


Fig. 11: Accuracy over the diffusion step t for different number of diffusion steps t using the optimal variance interval recorded in Figure 6: $\beta_1 = \beta_T = 10^{-4}$